EXPERIMENTAL ENVESTIGATION OF THE STRENGTH AND BEHAVIOR OF REINFORCED CONCRETE SPANDREL BEAMS UNDER REPEATED LOADS

Dr. Anis A. Mohamad-Ali and Dr. Adi Adnan Abdu-Alrazaq
University of Basrah-College of Engineering-Civil Engineering Department

ABSTRACT

The main objective of this study is to investigate the effect of repeated load on the strength and behavior of spandrel beam by considering eight specimens divided into four groups based on the design methods; type of cross section of the spandrel beam and the type of loading. Two design methods, two types of loading and two types of cross sections for spandrel beam are considered, the first is a solid rectangular section, while the other is a hollow rectangular section.

The effect of repeated loads on the cracks width, deflections, torque and the angle of twist is studied using two stages of loading, the first stage is at the soft-cracking stage after occurring of cracks in the spandrel beam and the second stage is the yielding of the bottom longitudinal reinforcement of the floor beam.

التحري المختبري لتحمل وتصرف عتبات الحافة الخرسانية المسلحة تحت تأثير الاحمال المتكررة

د. عدي عدنان عبد الرزاق – د. أنيس عبد الخضر محمد علي

جامعة البصرة – كلية الهندسة – قسم الهندسة المدنية

الخلاصة

يهدف هذا البحث إلى دراسة سلوك وتحمل عتبات الحافة الخرسانية المسلحة المعرضة إلى أحمال متكررة من القوى المتداخلة لكل من اللي والانثناء والقص. شمل البرنامج العملي فحص ثمانية نماذج تمثل عتبة أرضية–حافة مقسمة إلى أربعة مجاميع. حيث ان المتغيرات التي اعتمدها البحث هي : طريقة التصميم، طريقة التحميل، و شكل المقطع. حيث تم أتباع طريقتين لتصميم عتبة الحافة، مع اعتماد نوعين من التحميل، اضافة الى استعمال مقاطع مستطيلة مجوفة وأخرى صلدة لعتبة الحافة.

Introduction

The reinforced concrete civil engineering structures are designed to carry static loads in addition to dynamic loads which are either moving or movable and may vary with time.

Dynamic load can affect the strength of materials in only two ways; the first is related to rate of strain, when concrete is strained at a very rapid rate, its ultimate strength during that process is significantly higher than it would be at slower strain rates. This is true for yield stress of reinforcing steel. The second way, in which dynamic loading may affect the static strength of materials, is a failure due to action of repeated cycles of stress of lesser magnitude than would cause failure in a single loading. [1]

The available information about the effect of repeated loading on the reinforced concrete structures is very limited, so that, it's very interesting to study this effect, as a part of dynamic effect, on these structures specially on the members that are subjected to torsion forces with so large values that its effect cannot be neglected or overcome by applying certain safety factors to the shear design due to development of new structures such as spandrel beams in which the torsion is considered of primary importance together with flexural and shear.

The spandrel beam, as shown in (Fig. 1), lies at the edge of the frame and is connected by a joint to the floor beam, so that it's subject to compatibility torsion in addition to equilibrium torsion.

The strength and behavior of the floor-spandrel beam assembly has been investigated by many researches. The earliest which was presented by Saether and Prachand [2], where theoretical approach has been suggested to construct the interaction between the torsional deformation of the spandrel beams and the flexural bending adjoining slab and the supporting columns. Collins and Lampert [3] suggested that a zero torsional stiffness for the designing of the spandrel beam with providing a minimum torsional steel to insure ductility and to limit cracks. Hsu and Burton [4] attained that the spandrel beam may be assumed to carry a torsional stress of $0.33\sqrt{f'_c}$. This method was incorporated by the ACI-Code 1977 [5]. They proposed that the contribution of concrete to resist shear safely can be neglected in designing shear reinforcement of floor beam.

Tests made by Hsu on hollow and solid rectangular sections [6] indicated that concrete core did not contribute to the ultimate torsional strength of the solid beam. This true for wall thickness, t, greater than $\frac{b}{4}$, where b is the cross-sectional width, [7]. When the wall thickness is less than $\frac{b}{4}$, the strength of a hollow beam compared to companion solid beam is reduced. This reduction of strength is reflected by a factor $\frac{4t}{b}$. The minimum wall thickness for hollow beams is $\frac{b}{10}$.

Tests made by Mansure and Rangan [8], investigated that repeated loads has no significant effect on the ultimate strength, torque of spandrel beam assembly.

The present study aims to study the effect of repeated loads on the strength and behavior of the spandrel beam as a part of monolithic frame.

Test Program

The objective of the test program is to study the behavior of a floor-spandrel beam assembly under repeated loads at two different stages of loading. The first stage is the soft-cracking for both spandrel and floor beams, while the other is yielding of the bottom longitudinal reinforcement of floor beam.

Total of eight specimens were tested. The specimens were divided into four groups based on the type of cross section of the spandrel beam, design parameters, type of loading as shown in Table (1).

General Description

Figure (1) shows a three dimensional frame in which the floor-beam is framing into spandrel beam. When load, p, is applied to the floor beam, a rotation at the ends is produced which in turn induces a twisting moment in the spandrel beam. The interaction of floor beam and spandrel beam can be studied using the shaded portion in the shape of T-specimen in the plane which was separated at the inflection points as shown in the Fig. (2). This simplification was made due to difficulty and cost in testing three-dimensional frame. The existing condition at the cut sections may be simulated by appropriate hinges and restraint as shown in Fig. (3).

In this study, two types of loading have been used; the first is a single concentrated load at the mid-span of the floor beam (P) which represents the mid-span region of spandrel beam as shown in Fig. (4). The second is to apply an additional concentrated load at the joint (Ps) to simulate the condition of large shear force in the spandrel beam near the column as shown in Figs. (4 and 5). Where Ps = nP, and n is a constant equals to zero at the first case of the loading while it was assumed that constant equals to 0.5 at the second case of the loading.

Two design methods varying in estimating the value of the torsional moment is adopted in this study; the first which labeled (A) assumes that the

torsional stress is equal to ($0.33\sqrt{f'_c}$) [4], and the other is labeled (B) which assumes a zero torsional moment with a provision of minimum torsional reinforcement in the spandrel beam to insure ductility [3].

Table (2) gives the calculated shears and moments for the specimens. The longitudinal steel reinforcement to resist torsion in the spandrel beam was not provided because it has no significant effect on the torsional capacity, and the contribution of the concrete to resist shear was neglected in the designing of the stirrups of the floor beam up to distance, d, from the joint. This detailing was found to be more efficient and practical [9].

A certain detailing was provided in the joint between floor and spandrel beams, where the longitudinal steel reinforcement of the floor beam were extended longitudinally and placed over the longitudinal reinforcement of the spandrel beam with a 90 degree bend and vertically extended as shown in the Fig. (6) to provide the anchorage length required by the ACI-318 Building Code[10] to ensure adequate load transfer between the two beams across the joint.

In designing the spandrel beams, web reinforcement which determined to resist the shear and torsion stresses and the shear carried by the concrete, were computed according to the ACI 318-05 Building Code Requirements [10]. The floor beam as a flexural member was designed by the conventional method of designing flexural members.

Material Properties

The same concrete mix was used in all test specimens using ordinary Portland cement, sand and crashed gravel with maximum size of (10mm). The most suitable mixture was (1:1:2) and a water/cement ratio which gives acceptable workability was (0.45) with a slump of (75mm).

The properties of concrete and steel reinforcement that used in the study are listed in Tables (3) and (4), respectively. Ordinary deformed steel bars of different sizes were used for longitudinal reinforcement and mild steel plain bars for transverse reinforcement.

Fabrication

The hollow sections of the spandrel beams were achieved by using stirabore. The joint region was remaining solid to ensure that the failure occurred outside the joint region.

The floor-spandrel beam assembly was cast in a wooden mold which was lubricated with oil before placing the reinforcement. Continuous casting with no delay and compacting using electrical vibrator was carried out after placing the concrete. The specimens are cured after 24-hours when the sides of the wooden and steel molds were removed. They were covered with a hessian and continuously wetted for curing till the day before the test has been conducted.

Test Set-Up and Instrumentation

At the test, steel bearing balls were used to allow the ends of the spandrel beam to bend and twist. This ends were completely torsionally fixed by using steel torsional arms that are attached to each end of the beam as shown in Plate (1), while in the floor beam a steel cylinder bearing was used to allow the end of the beam to bend only.

A proving ring was fixed in between the torsional arm and a manually operated hydraulic jack in order to measure the torque induces in the spandrel beam through multiplying the readings of the proving ring (in terms of forces) by the length of the torsional arm.

The deflections of the mid-span of both spandrel and floor beams were measured using dial gauges. A rotational arm and two dial gages were used to measure the torsional rotation. The arm was fixed under the bottom face of the spandrel beam. One of the two dial gauges was placed under the arm in the mid-width of the spandrel beam (which is used to measure the deflection of the spandrel beam), while the other is placed at the other end of the

arm at distance (500mm). A measuring Microscope was used to measure the crack width.

The Arrangement of Cycles

The load was repeated at two stages. The first is the soft-cracking stage for both spandrel and floor beams. At this stage, the load was repeated using seven cycles. The second stage, at which the load was repeated, is after yielding of the bottom longitudinal reinforcement at the mid-span of floor beam where rapid increase in deflection was observed (plastic hinge stage). Numbers of cycles at these two stages are listed in Table (5). The cracking loads for both floor and spandrel beams are shown in Table (6).

Test Results and Behavior

Table (7) shows the measured loads and torques at failure. This table shows that for all specimens, the failure load is greater than that of design load. This is true for failure torque except for specimen GRB1. The measured failure loads and torques for load case (1) are greater compared to that of load case (2). This table shows that the measured failure loads for both hollow and solid sections are close, while the measured failure torques for solid sections are greater than that of hollow sections. Also, this table shows that the specimens that designed according to method (A) gives loads and torques at failure, under load case 1, greater than that of design method (B). While, for load case 2, the measured failure loads and torques are rather close for the two methods of design.

From the test, it is found that all specimens have the same behavior. So, the behavior of specimen GRA2 will be taken as an example to discuss the behavior of floor-spandrel beam assembly under repeated loads.

The flexural cracks for all specimens were first visible during the first load cycle at the mid-span of floor beam under the applied load at levels vary between (12% and 45%) of the ultimate load. Figure (7) shows the relationship between the applied load and deflection of floor beam under repeated load at soft-cracking stage for the specimen GRA2. The relationship between load and deflection, during the first cycle, behaves elastic linearly up to level of first visible cracks, after that, the curve starts to deviate from linearly. The cracks widen and extend slowly as the load increase. This trend continuous up to the level at which the load removed. This figure shows that the deflection decreases as the load decrease during the unloading path. At any load level of the unloading path, the deflection is greater than that of the loading path, but it is not vanished at the end of the load cycle. The width of flexural cracks, at the level of bottom longitudinal reinforcement of the beam, decreases with decreasing the load until it vanishes at the end of the load cycle.

The above behavior is true for the other next cycles. It can be seen from Fig. (7), that the values of deflection, at any load level, increase with increasing number of cycles. The values of maximum crack width are slightly affected by increasing number of cycles at soft-cracking stage, as shown in Fig. (8).

Figure (9) shows the load-deflection curve at the plastic hinge of floor beam stage. Behavior of the first cycle in this stage is quite similar to that of cycles in the soft cracking stage up to yield of the bottom longitudinal reinforcement in the mid-span of floor beam. Through this stage, wide cracks are developed as the tensile forces developed in concrete exceeding the concrete tensile strength. This occurs simultaneously with rapid increase in deflection, and this stills continuous up to the level at which the load remove. This figure shows that the initial part of the unloading path is unorganized, but later, it becomes nearly as a straight line along the unloading path. Deflections of the unloading path are greater than that of the loading path. At the end of this cycle, the crack widths reduce. The curves of the next load cycles behave linear for both loading and unloading paths. At any load level, the values of deflection increase with

increasing number of cycles, as it explained in the first stage of repeated loading. Figure (10) shows that the maximum crack widths are increased with increasing the number of cycles.

The Behavior of the final load cycle is similar to that of the previous cycles, as shown in Fig. (9). Further increase in loading, after yielding of the bottom longitudinal reinforcement, caused failure due to crashing of concrete in the compression zone after complete yielding of bottom steel.

Two types of cracks appear in the spandrel beam; the first type is the flexural cracks and the second is the torsional cracks. The flexural cracks are developed at the bottom of the outer face in the mid-span of the beam. The cracking load of such cracks varies from (29% to 59%) of the ultimate load. As the load increases, the cracks propagate vertically upward and then bend away from the center. The torsional cracks are developed first in the inner face of the spandrel beam with loading percentage varying from (14% to 53%) of the ultimate load. They propagate vertically for a short distance and then bend toward the joint.

Figure (11) shows that the behavior of load-deflection curve for spandrel beam at the first stage of repeated loading is same to that explained for floor beam at the same stage. But the values of deflection for the spandrel beam are less compared to that of floor beam.

Figure (12) shows the relationship between the applied load and the induced torque for spandrel beam, at soft-cracking stage, is linear up to level of load at which the first visible torsional cracks appear. After that, this curve deviate from linearly and this trend continue up to the level at which the load starts to remove. This is true for load-twist curve as shown in Fig. (13), indicating that all of the induced torsional moment before cracking is nearly resisted by the concrete. Both load-torque and load-twist curves behave linear along the unloading path.

Figures (11 to 13) show that after completely removing of the applied load, the torque in the spandrel beam vanishes, while the values of deflection and twist decrease but they are not vanishing.

It is found that, at any load level, the angle of twist is greater compared to that of the previous cycle, while the torque is smaller indicating that the contribution of concrete to resist torsion decreases gradually with increasing the number of cycles.

It was found from the test that width of the torsional cracks on the inside face of spandrel beam not vanished at the end of any load cycle on the contrary to the flexural crack width which vanishes at the end of the same cycle. At the same time, the repeated loading has a slight effect on the torsional and flexural cracks width as shown in Fig. (14).

Figures (15, 16 and 17) show the load-deflection, load-torque and load-twist, respectively, for the spandrel beam at the second stage of the repeated loading. These figures show that, at any load level, the values of deflection and twist for spandrel beam increase with increasing number of cycles, while the values of the induced torque are decreased.

Figure (18) shows that the repeated load at the second stage has a slight effect on the torsional and flexural cracks width.

It can be concluded that the behavior of spandrel beams under repeated loading after yielding of the bottom longitudinal steel in floor beam mainly depends on the ratio of the maximum imposed load per cycle to the ultimate load, stirrups and number of cycles.

It is found that for all specimens, the ultimate load is reached when a considerable drop in torque with rapid increase in the angle of twist have been occurred and the concrete on the top face of spandrel beam close to the joint is crushed.

Conclusions

The following conclusions can be drawn from this study:

1- Repeated loading leads to reduce the torsional resistance of the concrete. This resistance may vanish when the load is repeated at so high maximum levels that they lead to yielding of the longitudinal steel of the floor beam. As a result, twists become larger and crack width becomes wider, so the concrete can not contribute to resist the applied torque. Then, all the applied torque would be resisted by stirrups, thus the torsional capacity of the spandrel beam depending on the stirrups.

2- Using the limit design concept proposed by Hsu and Burton [4] for beams under repeated loads is found to be satisfactory for the entire length of the spandrel beam. This method is desirable as it yields an economic design.

3- The ACI-Code provisions, in treating the box section, have a good agreement with the test result. These provisions can be used satisfactorily.

5- Transverse steel has no influence on the beam prior to cracking. But it has a significant effect on the ultimate strength and the behavior of specimens in the post-cracking stage.

6- The presence of high shear stress, as in the case of two concentrated loads, leads to wider cracks on the inside face of the spandrel beam where stresses due to shear and torsion are additive. Also, this type of loading leads to larger deflections of spandrel beams compared to that of beams with normal shear, while no visual effect on the deflections of floor beam is observed.

References

1- Charles H. Norris: "Structural Design for Dynamic Loads", McGraw-Hill Civil Engineering Series, 1959, pp.20.

2- Saether, K. and Prachand, N. M., "Torsion in Spandrel Beam", ACI Journal, Vol. 66, No. 1, January 1969, pp. 24-30.

3- Collins, M.P. and Lampert, P.; "Redistribution of Moments at Cracking-The Key to Simpler Torsion Design", Analysis of Structural Systems for Torsion, ACI publications, SP-35, Detroit, 1973, pp.343-384.

4- Hsu, T.T.C., and Burton, K. T.; "Design of Reinforced Concrete Spandrel Beam", Journal of Structural Division, Proc. of ASCE, Vol. 100, No.St1, January 1974, pp.209-229.

5- American Concrete Institute; "Building Code Requirement for Reinforced Concrete", ACI 318-77, Detroit, October 1977.

6- Hsu, T.T.C.; "Torsion of Structural Concrete-Behavior of Reinforced Concrete Rectangular Members", Special Publications, Sp-18, ACI, Detroit, 1968.

7- Hsu, T.T.C.; "Background and Practical Application of Tentative Design Criteria for Torsion", ACI Structural, Journal, Vol. 66, No. 1, January, 1969, pp. 12-23.

8- Mansur, M. A. and Rangan, B. V.; "Repeated Loading of Reinforced Concrete Spandrel Beams", The University of New South Wales Sydney, Australia, Pres, Reinforced Concrete Component, 1981, pp. 323-341.

9- Mohamad Ali, A.A.; "Strength and Behavior of Reinforced Concrete Spandrel Beam", Ph.D. Thesis, University of Edinburgh, 1983.

10- American Concrete Institute; "Building Code Requirements for Reinforced Concrete", ACI 318-05, Detroit, November 2005.

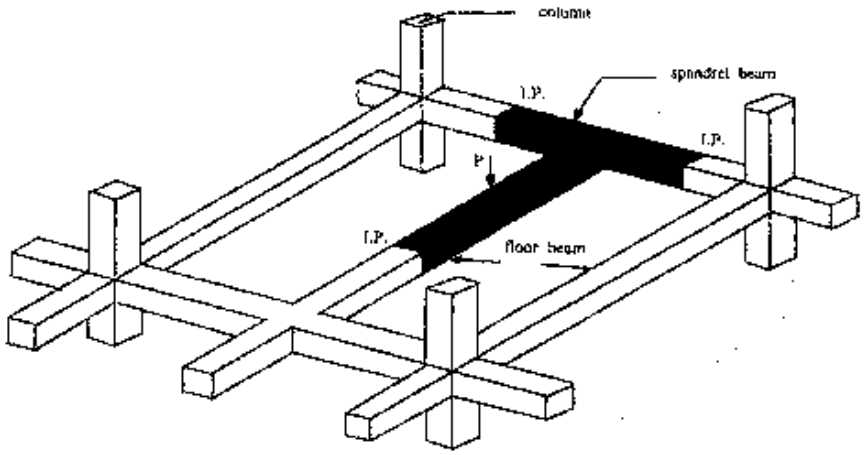

Fig. (1): Spandrel Beam with A Structural Frame.

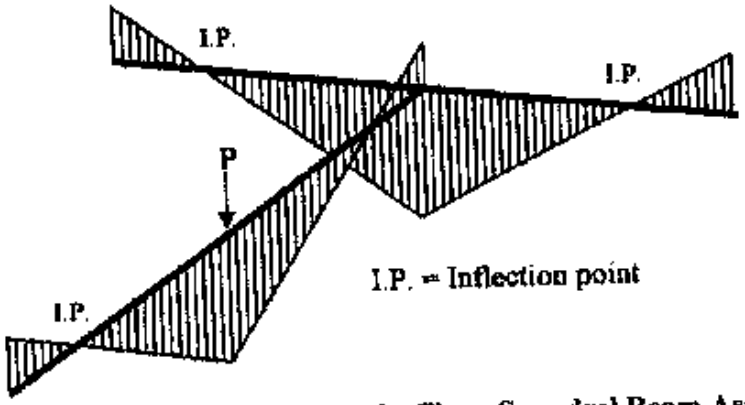

Fig. (2): Bending Moment Diagram for the Floor-Spandrel Beam Assembly under Load, P.

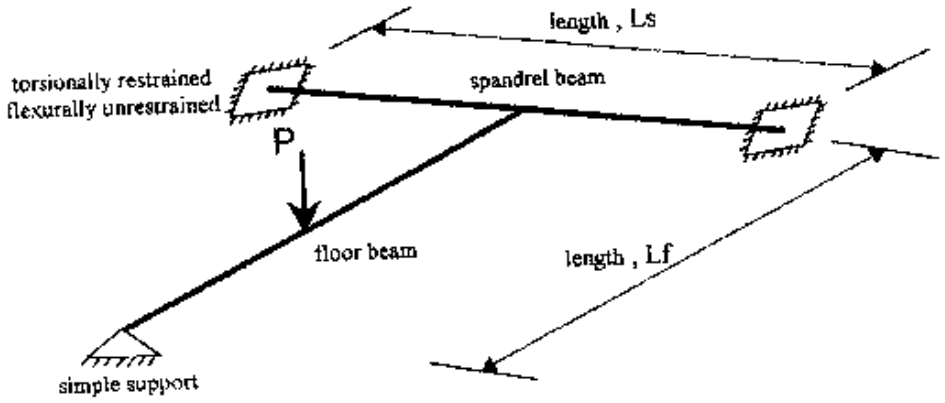

Fig. (3): Structural Model for the Floor-Spandrel Beam Assembly.

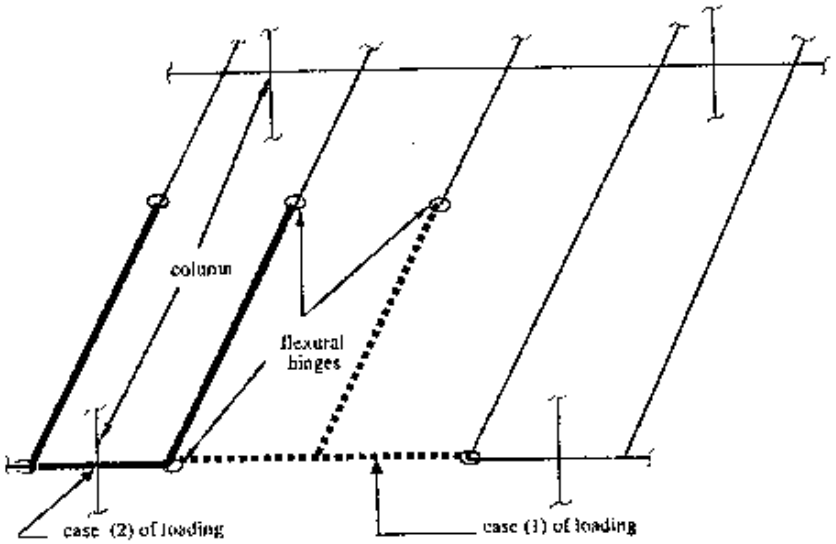

Fig. (4): Actual Conditions of Loading in Frame.

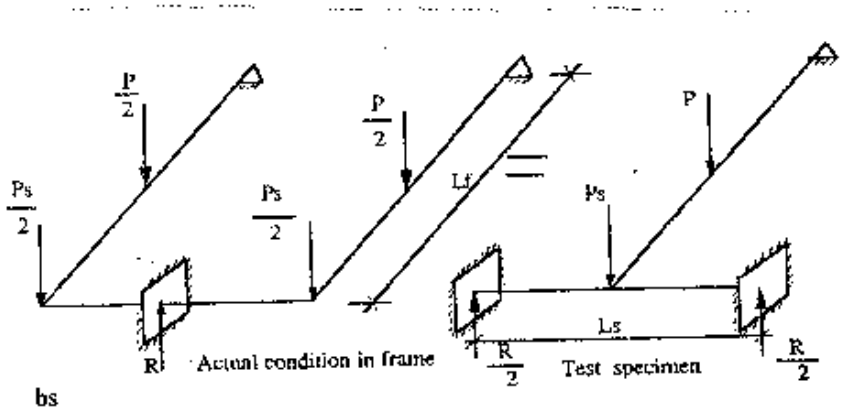

Fig. (5): Simulation of the Second Case of Loading.

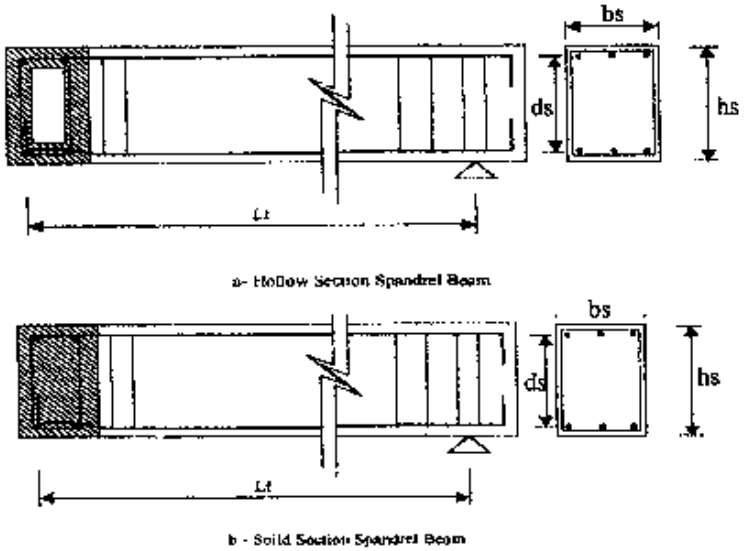

Fig. (6): Typical Reinforcement Details (Spandrel Beam Shaded).

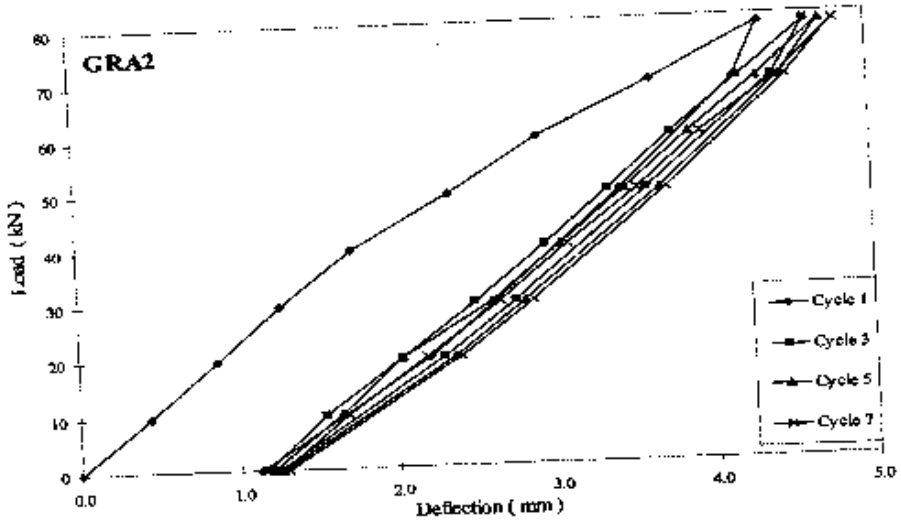

Fig. (7): Load-Deflection at mid-Span of F. Beam Curve at Soft-Cracking Stage for Specimen GRA2.

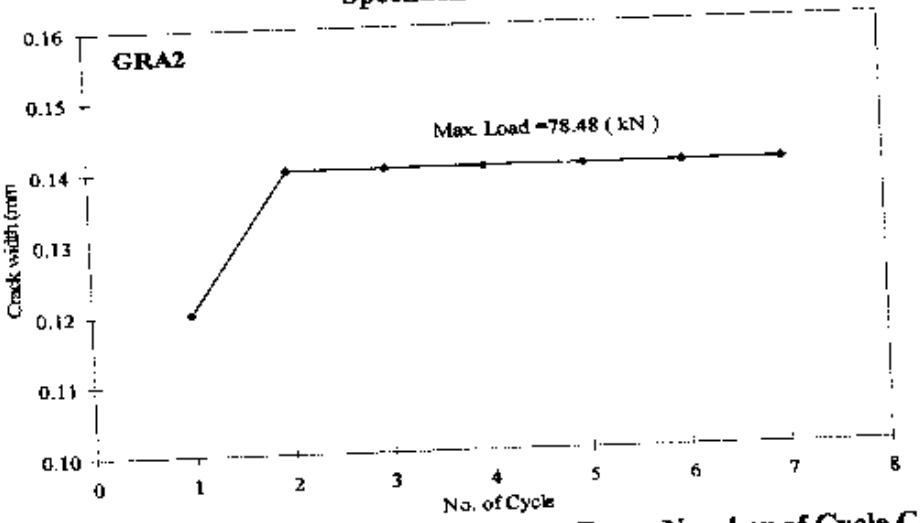

Fig. (8): Max. Flexural Crack Width of Floor Beam-Number of Cycle Curve in the Soft-Cracking Stage for Specimen GRA2.

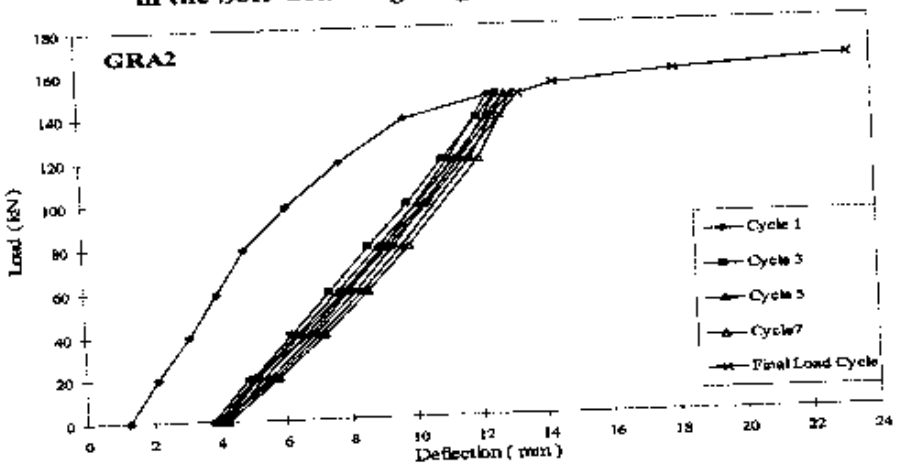

Fig. (9): Load-Deflection at mid-Span of F. Beam Curve at Plastic Hinge Stage for Specimen GRA2.

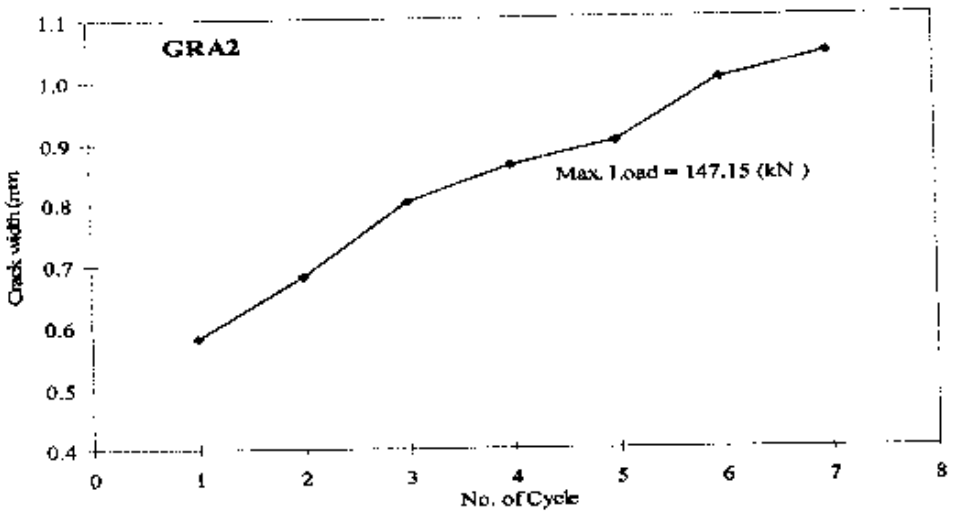

Fig. (10): Max. Flexural Crack Width of Floor Beam-Number of Cycle Curve in the Plastic Hinge Stage for Specimen GRA2.

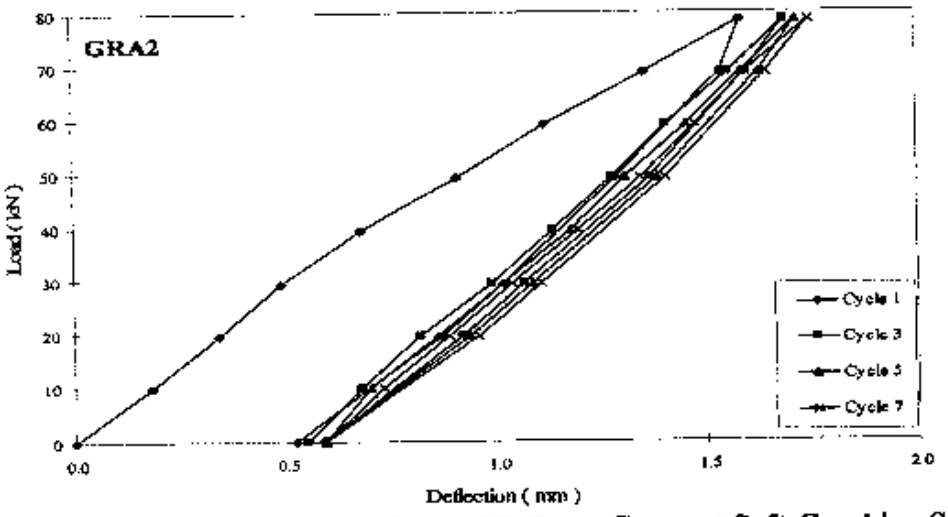

Fig. (11): Load-Deflection at mid-Span of S. Beam Curve at Soft-Cracking Stage for Specimen GRA2.

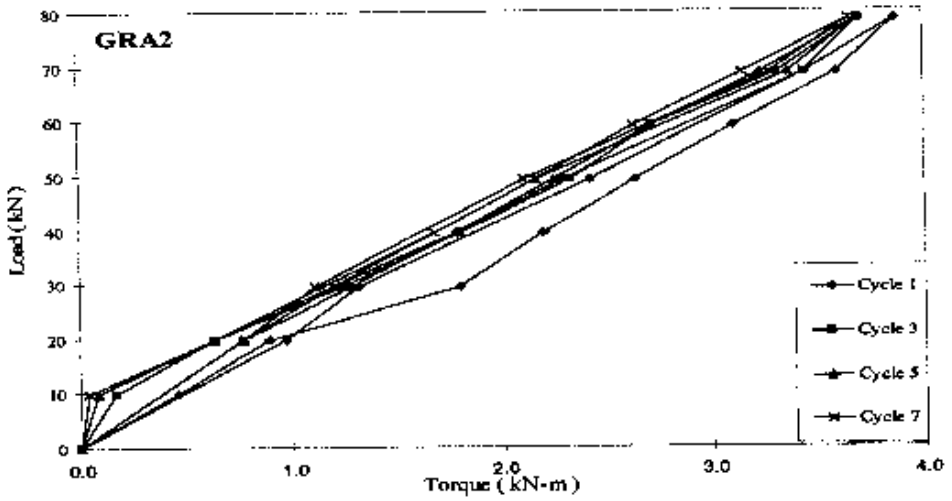

Fig. (12): Load-Torque of S. Beam Curve at Soft-Cracking Stage for Specimen GRA2.

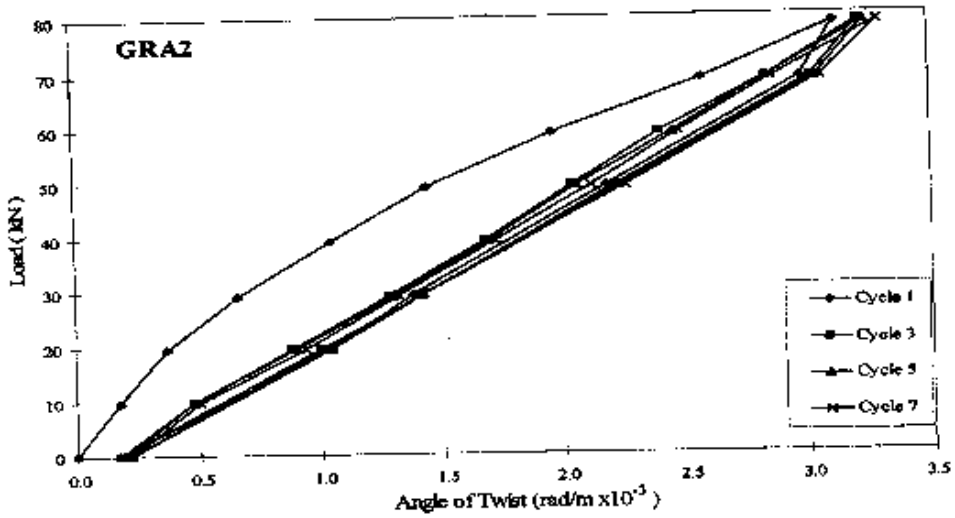

Fig. (13): Load-Angle of Twist of S. Beam Curve at Soft-Cracking Stage for Specimen GRA2.

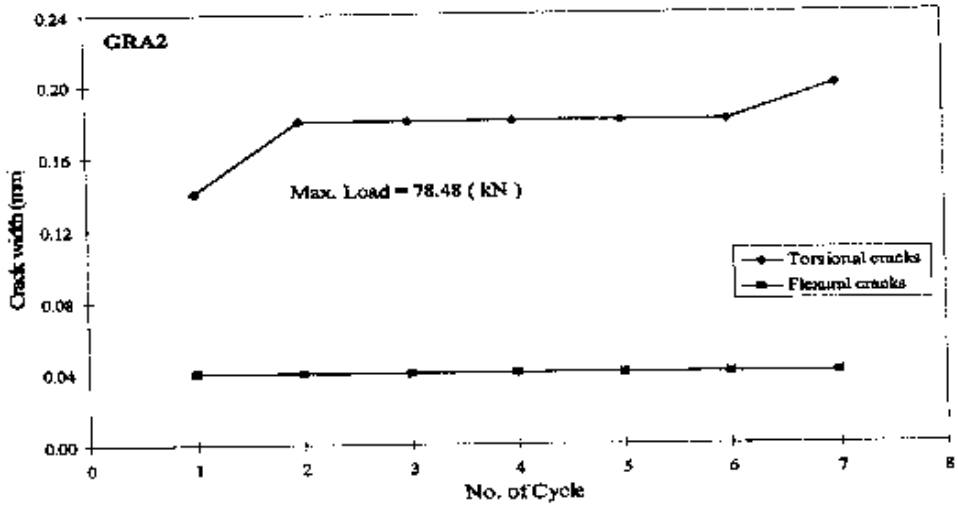

Fig. (14): Max. Crack Width of S. Beam-Number of Cycle Curve at the Soft-Cracking Stage for Specimen GRA2.

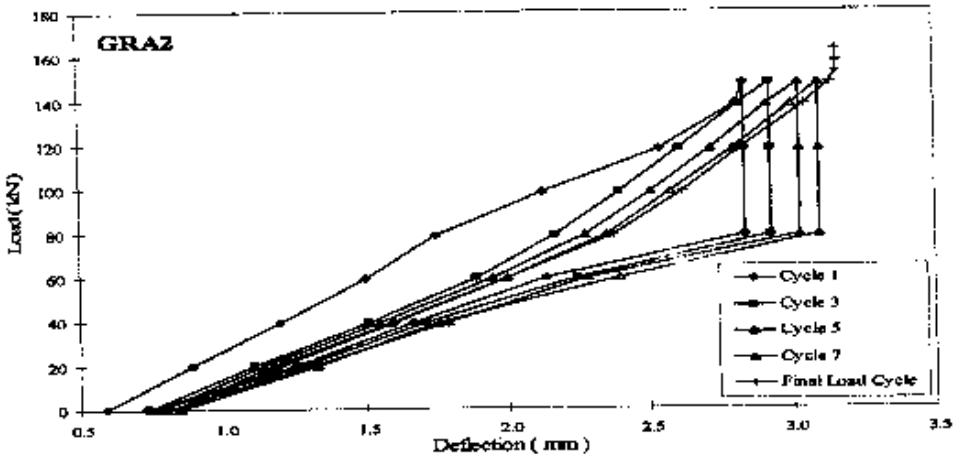

Fig. (15): Load-Deflection at mid-Span of S. Beam Curve at Plastic Hinge Stage for Specimen GRA2.

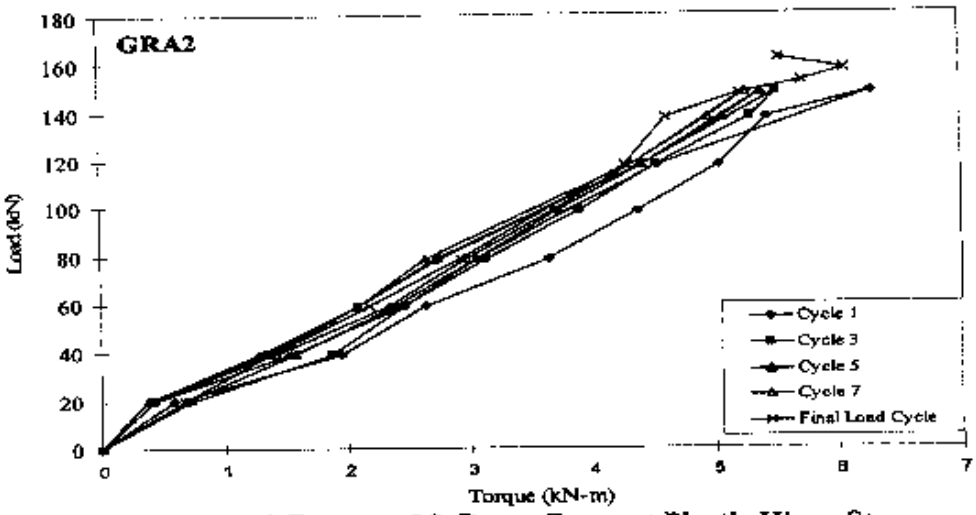

Fig. (16): Load-Torque of S. Beam Curve at Plastic Hinge Stage for Specimen GRA2.

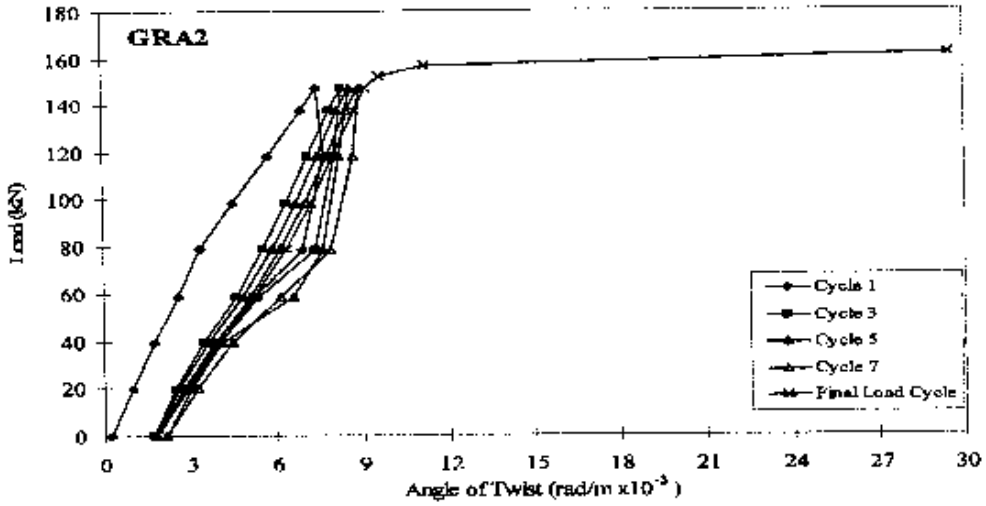

Fig. (17): Load-Angle of Twist of S. Beam Curve at Plastic Hinge Stage for Specimen GRA2.

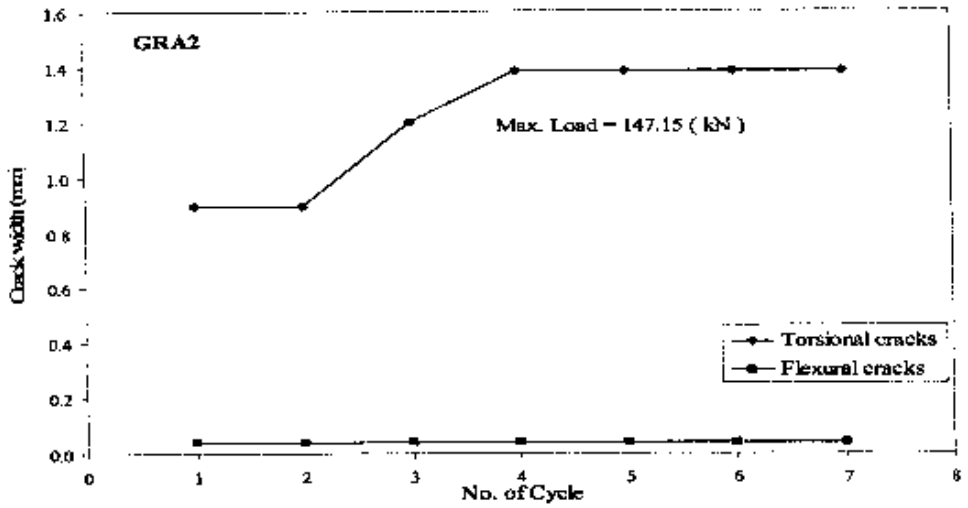

Fig. (18): Max. Crack Width of S. Beam-Number of Cycle Curve at Plastic Hinge Stage for Specimen GRA2.

Plate (1): Torsional Arm Arrangement.